Simulation and Analysis of Chaotic Rössler System based on Circuits

Juan S. Cárdenas R.
Student
Universidad EAFIT
Medellín, Colombia
jscardenar@eafit.edu.co

David Plazas E.
Student
Universidad EAFIT
Medellín, Colombia
dplazas@eafit.edu.co

***Abstract*—In this work, the Rössler system is studied: a short introduction about the history of the system is given, as well as some state-of-the-art applications; a circuit implementation is presented based on previous work; a simulation diagram is proposed for the obtained dynamic equation and used to acquire results. A validation is done with known results in the literature and then proceeded to tweak the system, in both input and parameters, in order to analyze its response through time and determine intervals for the parameters such that the system remains chaotic. The results obtained only allowed us to determine enclosing intervals for these parameters, since a more detailed study must be done in order to determine exact values.**

***Index Terms*—Rössler attractor, chaos, numerical solution, simulation, state equation, dynamic system, chaotic circuit.**

I. Introduction

The system in study was proposed by O.E. Rössler in 1976, as a simplified model with shape and behavior similar to spirals in Lorenz system, which was not fully understood at the time due to the techniques known to study oscillators were not applicable to Lorenz model [1]. The Rössler equations are:

$$\begin{aligned} \dot{x} &= -y - z \\ \dot{y} &= x + ay \\ \dot{z} &= b + z\left(x - c\right) \end{aligned} \tag{1}$$

Although Rössler affirmed that the system did not have immediate physical interpretation [1], nowadays some applications can be found using the model as a mechanism and not as an abstraction of a physical system. The model presented has been used as a tool for image cryptography as it was shown by Mandal *et al.* in [2]; in further work, Laiphrakpam and Khumanthem proposed improvements to Mandal's algorithm, as it is shown in [3]. On the other hand, coupled Rössler system with different inputs have been used to measure the correlation of time series, as Weule *et al.* showed in [4].

In order to bring the system to the real world, Rössler equations can be represented by a circuit, as Canals *et al.* show in [5]. The proposed circuit is shown in Fig. 1 and can be translated to

$$\begin{aligned} RC\dot{x} &= -y - z \\ RC\dot{y} &= x + ay \\ RC\dot{z} &= b + z\left(x - c\right) \end{aligned} \qquad \begin{aligned} a &= \frac{100k\Omega}{R_a} \\ b &= V_{cc}\frac{100k\Omega}{R_b} \\ c &= \frac{100k\Omega}{R_c} \end{aligned} \tag{2}$$

In [5] they use this circuit to generate true random numbers using the output of the voltage of the node z. The nodes x and y have a fixed frequency of oscillation if the other variable is set to 0, since their rate of change are linear. In contrast, z induces chaos to the circuit, due to its nonlinear behavior. In this manner, this variable was selected to be the output as its chaotic behavior is useful to generate random numbers [5].

Therefore, in this paper will study the question: "Which interval of values for the supplied voltages and resistances in the circuit can preserve the chaos of the system?". It is conjectured that with small values of the resistance, the system will reach their maximum charge quicker than the simulation period, therefore it will stabilize and won't show chaotic behaviour. Otherwise, with the voltages supplied by the battery, it is hypothesized that for larger values the circuit would reach the maximum charge quicker so it will not be chaotic either.

In order to answer this question, the system will be simulated with different types of inputs, so it can be analyzed how the circuit behaves if the battery supplies different voltages to the system. Lastly, two parameters will be changed so it can be observed how the system acts with different resistance values, in order to find a interval where the system still has chaotic behaviour.

In section II, the dynamic equation can be found, as well as the numerical algorithms to simulate the system. In section III, the results of the simulations with different types of inputs and parameters. In section IV, the analysis of the obtained results and their justification. Lastly, the conclusions of the work are presented in section V.

II. Methods

A. Dynamic System

In the circuit presented, according to Canals *et al.* [5], the variables x, y and z represent the voltages through the nodes shown in Fig. 1. The RC parameter defines the system's time (in seconds), the supplied voltages are $V_{cc} = 15V$ and $V_{ss} = -15V$; R_a, R_b y R_c are resistors in $k\Omega$ used to calculate the system's original parameters, as shown in (2). In order to simulate the system in Simulink, the state and output equations will be used; thus, the dynamic equation is given by

$$\begin{cases} \dot{x_1} = \dfrac{1}{RC}\left(-x_2 - y\right) \\ \dot{x_2} = \dfrac{1}{RC}\left(x_1 + \dfrac{100k\Omega}{R_a}x_2\right) \\ \dot{x_3} = \dfrac{1}{RC}\left[\left(V_{cc0} + u\left(t\right)\right)\dfrac{100k\Omega}{R_b} + y\left(x_1 - \dfrac{100k\Omega}{R_c}\right)\right] \\ y = x_3 \end{cases} \tag{3}$$

where y is the output and u the input; note that the parameter V_{cc} was selected as input, thus we select an initial value V_{cc0} and add the input $u\left(t\right)$ in Volts. For the rest of this document, the state variable x_3 will be referred as y, since it has been chosen as the output.

B. Implementation using Simulink

Using equation system (3), a simulation diagram was constructed using Simulink, as Fig. 2 shows.

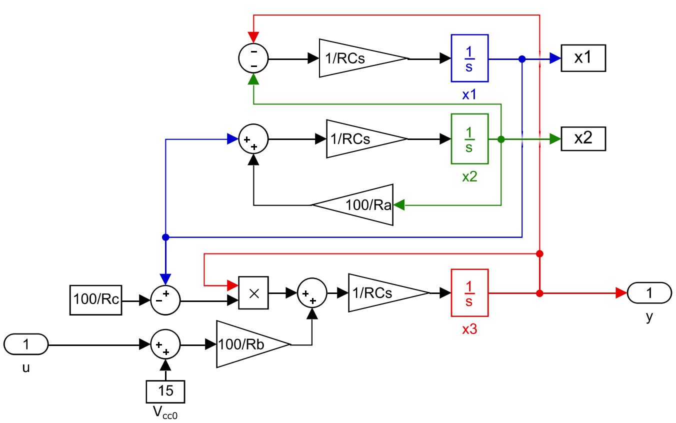

Figure 2: Simulation diagram for Rössler system.

C. Numerical algorithms

Given the differential equation to solve:

$$\dot{x} = f\left(t, x\right) \tag{4}$$

With the initial condition $x\left(0\right) = x_0$ and a step of time h that discretize the system. The simulation for the solution of x can be obtained with different methods such as Runge-kutta and Euler. This algorithms and more can be found in [6]. Note that the following methods will have implicit sample time.

1) Euler: Using Euler's method, the difference equation is:

$$x\left(k+1\right) = x\left(k\right) + hf\left(k, x\left(k\right)\right) \tag{5}$$

2) Runge-kutta: In the fourth order Runge-Kutta's method, the difference equation is:

$$x\left(k+1\right) = x\left(k\right) + \frac{h}{6}\left(k_1 + 2k_2 + 2k_3 + k_4\right) \tag{6}$$

Where:

$$\begin{aligned} k_1 &= f\left(k, x\left(k\right)\right) \\ k_2 &= f\left(k + \frac{h}{2}, x\left(k\right) + \frac{hk_1}{2}\right) \\ k_3 &= f\left(k + \frac{h}{2}, x\left(k\right) + \frac{hk_2}{2}\right) \\ k_4 &= f\left(k + h, x\left(k\right) + hk_3\right) \end{aligned} \tag{7}$$

For the system in study, the difference equations are:

$$\mathbb{X}\left(j+1\right) = \mathbb{X}(j) + \frac{h}{6}\left(\mathbb{K}_1 + 2\mathbb{K}_2 + 2\mathbb{K}_3 + \mathbb{K}_4\right) \tag{8}$$

Where:

$$\mathbb{X}(j) = \left[x_1(j) \quad x_2(j) \quad y(j)\right]^T \quad \mathbb{K}_i = \left[k_{ix_1} \quad k_{ix_2} \quad k_{iy}\right]^T$$

Then, we have:

$$\begin{aligned} k_{1x_1}(j) &= -x_2(j) - y(j) \\ k_{1x_2}(j) &= x_1(j) + \frac{100}{R_a}x_2(j) \\ k_{1y}(j) &= \left[V_{cc0} + u(j)\right]\frac{100}{R_b} + \left(x_1(j) - \frac{100}{R_c}\right)y(j) \end{aligned}$$

$$\begin{aligned} k_{2x_1}(j) &= -\left(x_2(j) + \frac{hk_{1x_1}(j)}{2}\right) - \left(y(j) + \frac{hk_{1x_1}(j)}{2}\right) \\ k_{2x_2}(j) &= \left(x_1(j) + \frac{hk_{1x_2}(j)}{2}\right) + \frac{100}{R_a}\left(x_2(j) + \frac{hk_{1x_2}(j)}{2}\right) \\ k_{2y(j)} &= \left[V_{cc0} + u(j)\right]\frac{100}{R_b} \\ &\quad + \left[\left(x_1(j) + \frac{hk_{1y}(j)}{2}\right) - \frac{100}{R_c}\right]\left(y(j) + \frac{hk_{1y}(j)}{2}\right) \end{aligned}$$

$$\begin{aligned} k_{3x_1}(j) &= -\left(x_2(j) + \frac{hk_{2x_1}(j)}{2}\right) - \left(y(j) + \frac{hk_{2x_1}(j)}{2}\right) \\ k_{3x_2}(j) &= \left(x_1(j) + \frac{hk_{2x_2}(j)}{2}\right) + \frac{100}{R_a}\left(x_2(j) + \frac{hk_{2x_2}(j)}{2}\right) \\ k_{3y}(j) &= \left[V_{cc0} + u(j)\right]\frac{100}{R_b} \\ &\quad + \left[\left(x_1(j) + \frac{hk_{2y}(j)}{2}\right) - \frac{100}{R_c}\right]\left(y(j) + \frac{hk_{2y}(j)}{2}\right) \end{aligned}$$

$$\begin{aligned} k_{4x_1}(j) &= -\left(x_2(j) + hk_{3x_1}(j)\right) - \left(y(j) + hk_{3x_1}(j)\right) \\ k_{4x_2}(j) &= \left(x_1(j) + hk_{3x_2}\right) + \frac{100}{R_a}\left(x_2(j) + hk_{3x_2}\right) \\ k_{4y}(j) &= \left[V_{cc0} + u(j)\right]\frac{100}{R_b} \\ &\quad + \left[\left(x_1(j) + hk_{3y}\right) - \frac{100}{R_c}\right]\left(y(j) + hk_{3y}\right) \end{aligned}$$

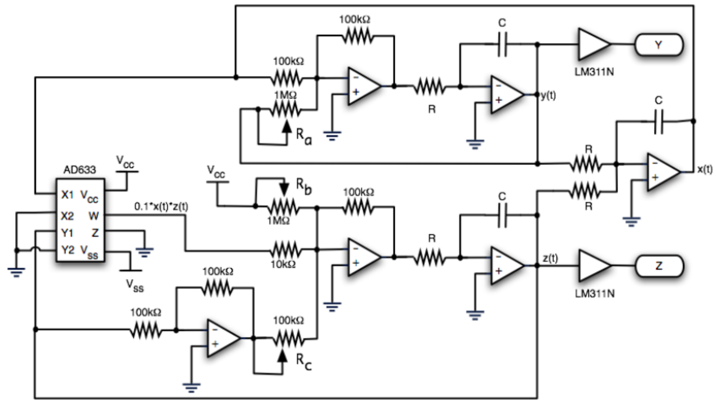

Figure 1: Rössler circuit representation [5].

III. Results

All the following simulations were implemented in Simulink, using fourth order Runge-Kutta algorithm with fixed step size of 0.001.

A. Model Validation

Before proceeding with further analysis, the model in analysis must be tested and compared with known results.

The comparison will be done with 2 different authors. First, Rössler original paper [1, Fig. 2] will be used as reference. Rössler firstly proposed the model using $a = b = 0.2$ and $c = 5.7$ with initial conditions $(x_{10}, x_{20}, y_0) = (0, -6.78, 0.02)$. Thus, the parameters for our circuit simulation will be $u(t) = 0V$, $V_{cc0} = 15V$, $RC = 1s$, $R_a = 500k\Omega$, $R_b = 7500k\Omega$, $R_c = 17.5934k\Omega$, with $t_0 = 0s$ and $t_{\text{end}} = 339.249s$. The results of the simulation are shown in Fig. 3.

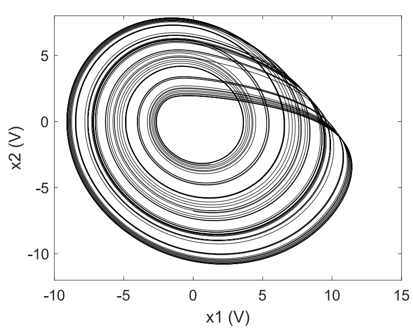

Figure 3: Phase portrait results of $x_2 x_1$ plane using Rössler [1] parameters.

This figure shows the trajectory followed by the system between $t = 0$ and $t = 339.249$, note that it follows an enclosed trajectory but not necessarily periodic; note as well the Möbius strip-like behavior, as Rössler states in his main paper [1].

On the other hand, Sprott and Li presented useful simulations for Rössler system, providing results for both phase portraits and time responses of the state variables [7, Figs. 2 and 3]. The simulations were done with $a = 0.29$, $b = 0.14$ and $c = 4.52$, with two initial conditions: $IC1 = (-1.25, -0.72, -0.10)$ and $IC2 = (0.72, 1.28, 0.21)$. Thus, our circuit parameters are $u(t) = 0V$, $V_{cc0} = 15V$, $RC = 1s$, $R_a = 344.8276k\Omega$, $R_b = 10714k\Omega$, $R_c = 22.1239k\Omega$, with $t_0 = 0s$ and $t_{\text{end}} = 100s$.

The results for the phase portraits are shown in Fig. 4 and for the time responses in Fig. 5.

B. Input Variations

For comparing the results, we will be using the original Rössler model initialization [1] as a reference and this simulation will be used for comparison. The parameters are $u(t) = 0V$, $V_{cc0} = 15V$, $RC = 1s$, $R_a = 500k\Omega$, $R_b = 7500k\Omega$, $R_c = 17.5439k\Omega$, with $t_0 = 0s$, $t_{\text{end}} = 100s$ and initial conditions $(x_{10}, x_{20}, y_0) = (0, -6.78, 0.02)$. For all the following simulations, only the 3D plot for the state variables and the output response in time will be presented. In Figs. 6 and 7 the reference simulation results are presented. Three different inputs were selected according to our input definition: two sine waves and a step in the V_{cc} voltage.

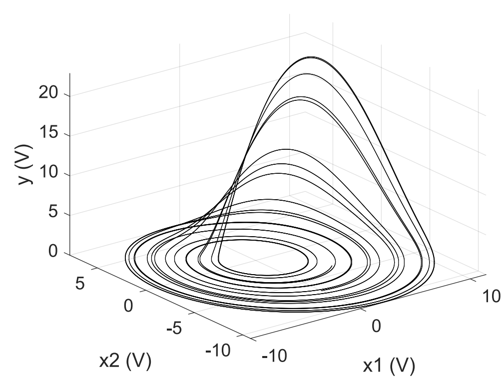

Figure 6: 3D plot for the state variables and the output for reference Rössler attractor.

It is important to highlight that the behavior showed in Fig. 7 is a good example of the response that Canals *et al.* [5] affirmed: the peaks in the output signal are unpredictable in time (this does not imply that the system is unpredictable).

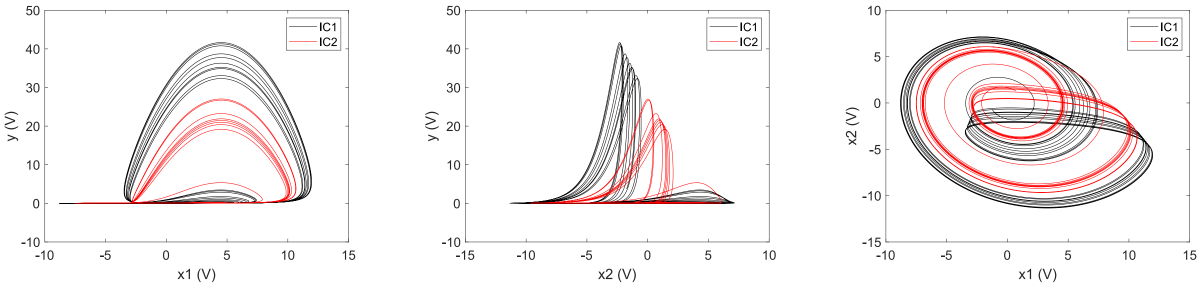

Figure 4: Phase portraits for the state variables with $IC1$ and $IC2$ as initial conditions.

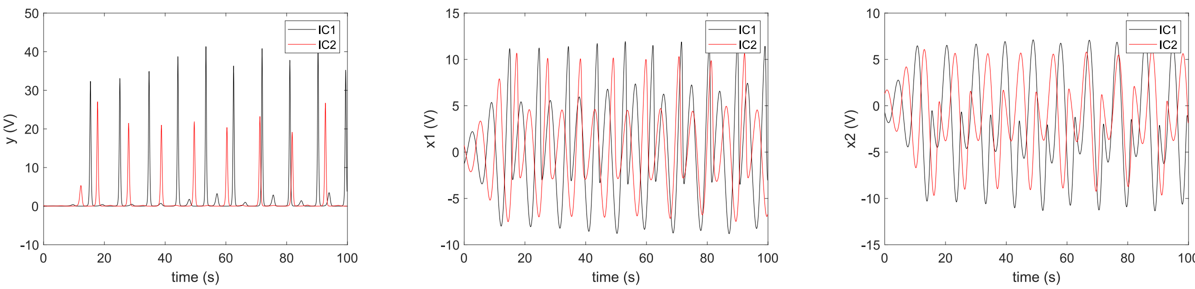

Figure 5: Time responses for signals y, x_1, x_2 with initial conditions $IC1$ and $IC2$.

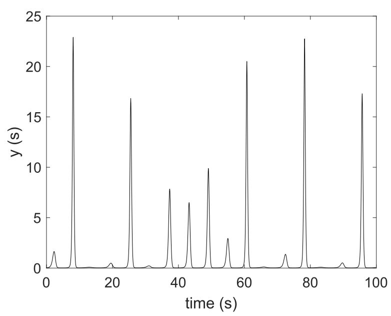

Figure 7: Output signal in time for reference Rössler attractor.

1) Sines Inputs: First, a sine wave with frequency $\omega = 2\text{rad} * s^{-1}$, amplitude $A = 500V$ and offset of $b = 500V$. Thus, the input is

$$u(t) = (500V)\sin(2t) + 500V \tag{9}$$

The plot for this input is shown in Fig. 8. The system's response is shown in Figs. 9 and 10.

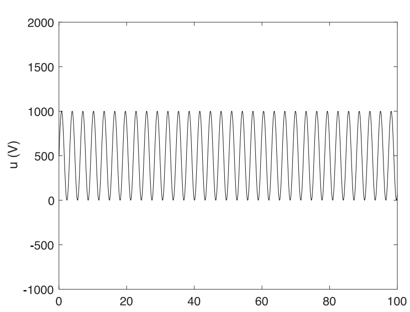

Figure 8: Input sine wave with $\omega = 2\text{rad} * s^{-1}$.

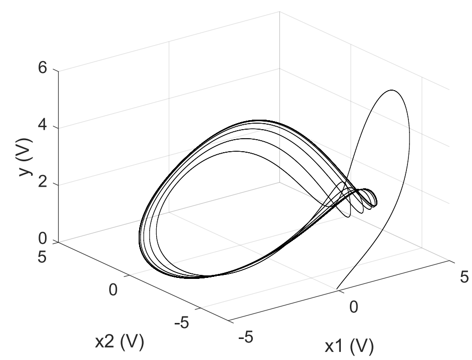

Figure 9: Phase portrait for the three state variables with sine input.

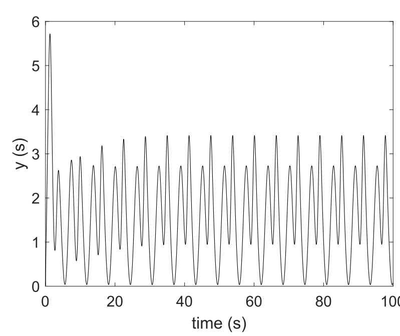

Figure 10: Output signal response in time for sine input.

Notice that eventually the trajectory falls in a closed and periodic orbit; as expected, the output signal is periodic but first modulated by an increasing signal.

Second, a sine wave with frequency $\omega = 5\text{rad} * s^{-1}$, amplitude $A = 500V$ and offset of $b = 500V$. Thus, the input is

$$u(t) = (500V)\sin(5t) + 500V \tag{10}$$

The plot for this input is shown in Fig. 11. The system's response is shown in Figs. 12 and 13.

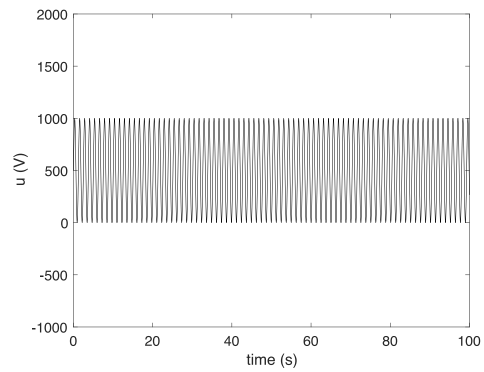

Figure 11: Input sine wave with $\omega = 5\text{rad} * s^{-1}$.

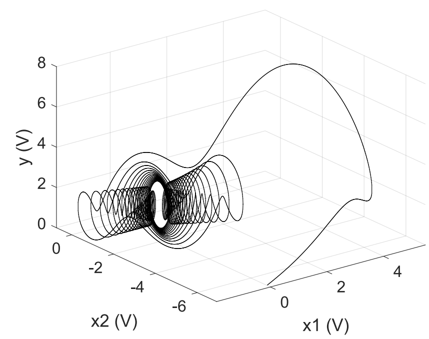

Figure 12: Phase portrait for the three state variables with sine input.

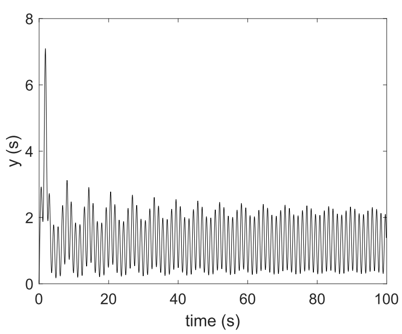

Figure 13: Output signal response in time for sine input.

As well as the previous sine input, the system falls into a periodic orbit first decreases its amplitude. The output signal is periodic but modulated by a decreasing signal.

2) Step: The step input was selected with step time of $40s$, initial value of $0V$ and final value of $1000V$. Hence, the input is given by

$$u(t) = (1000V)H(t - 40s) \tag{11}$$

Where $H(t)$ is the Heaviside step function. Fig. 14 shows the step input and Figs. 15 and 16 show the simulation results.

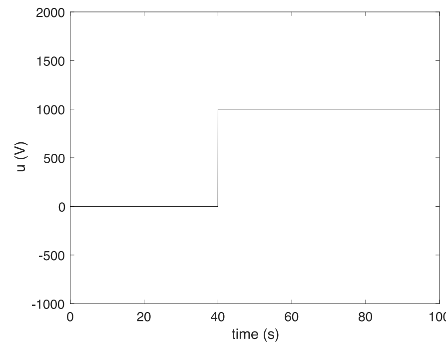

Figure 14: Step input.

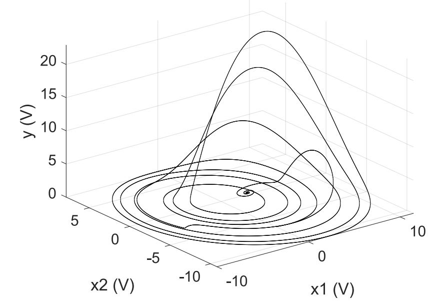

Figure 15: 3D phase portrait for x_1, x_2 and y

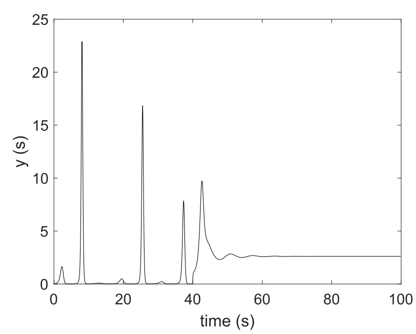

Figure 16: Output signal response in time for step input.

The 3D plot for the state variables shows that it starts normally as the Rössler attractor, but once the input is applied, the system stabilizes in completely, converging to an specific point in space. In the output signal through time the stability is evidenced in the constant value for y.

C. Parameter Variation

In this section, several simulations were made varying the values for parameters R_a and R_c, choosing values with important impact in the system's response. All simulations were made assuming $u(t) = 0V$, $V_{cc0} = 15V$, $RC = 1s$, $R_a = 500k\Omega$, $R_b = 7500k\Omega$, $R_c = 17.5439k\Omega$, with $t_0 = 0s$, $t_{\text{end}} = 100s$ and initial conditions $(x_{10}, x_{20}, y_0) =$

$(0, -6.78, 0.02)$. Keep in mind that, when a parameter is selected to vary, the rest of the parameters, initial conditions and solution method remains the same.

It is important to highlight that R_b was not chosen for the parameter variation since varying it is similar to changing the input for the system.

1) Parameter R_a: For parameter R_a, higher values from the reference $R_a = 500k\Omega$ were selected, since smaller values than the reference produces behaviors similar enough with the reference system (Figs. 6 and 7), even though there is a point where the response changes completely; this result will be presented in section III-D1. The selected values for the parameter are $R_{a_1} = 650k\Omega$, $R_{a_2} = 750k\Omega$, $R_{a_3} = 1750k\Omega$ and $R_{a_4} = 3652k\Omega$. The results are shown in Figs. 17 and 18.

2) Parameter R_c: Following the procedure of the previous section, both increments and smaller values of R_c have been selected to evidence the response of the system. For the smaller values $R_{c_1} = 10k\Omega$, $R_{c_2} = 5k\Omega$, $R_{c_3} = 2k\Omega$ and $R_{c_4} = 1k\Omega$ have been selected. The results for the simulations with this parameters are shown in Figs. 19 and 20.

For greater values, $R_{c_5} = 10k\Omega$, $R_{c_6} = 5k\Omega$, $R_{c_7} = 2k\Omega$ and $R_{c_8} = 1k\Omega$ were selected. The simulation results are shown in Figs. 21 and 22.

D. Limit for Parameter Variation

In the following simulations, extreme values for R_a and R_c are presented; that is, values for which the output y starts to behave unaccordingly. The values presented here were found following a bisection method, between a known normal behavior for the system and a point where the derivative in the simulation was not finite.

1) Parameter R_a: First, a significantly close value to the minimum for R_a was obtained around $259.098131084k\Omega$. In Figs. 23 and 24 the behavior of the output in time and all three variables is shown.

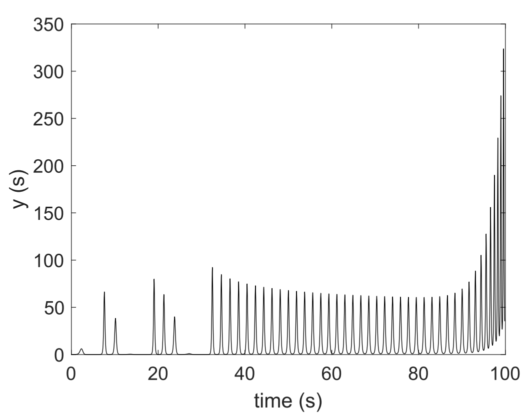

Figure 23: Output signal in significant time for reduction in parameter R_a.

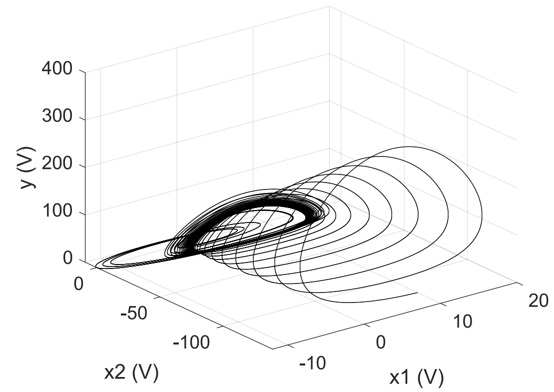

Figure 24: 3D phase plot for the state variables for a significant reduction in parameter R_a.

Notice that, in the three-dimensional plot for the state variables, the trajectory starts to separate from the attractor; in the graph of y against time, the output signal explodes and as t increases, the output tends to infinity.

Second, R_a was set to $10000k\Omega$; this value was not found with the bisection method, since R_a can take arbitrarily large numbers and all show the same output. In Figs. 25 and 26 the behavior of the output in time and all three variables is shown.

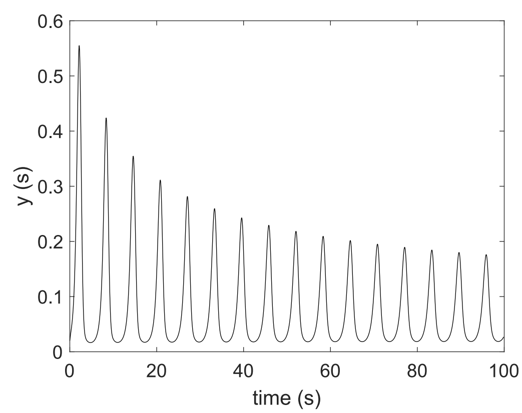

Figure 25: Output signal in time for a significant increment in parameter R_a.

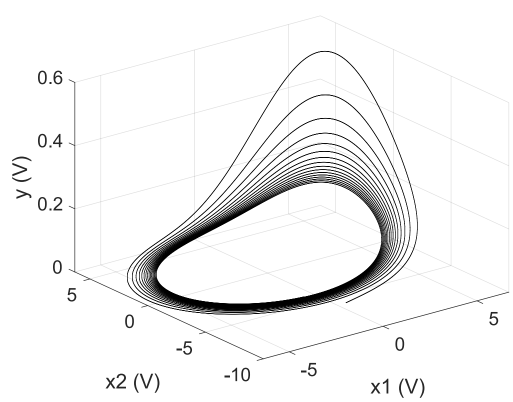

Figure 26: 3D phase plot for the state variables for an increment in parameter R_a.

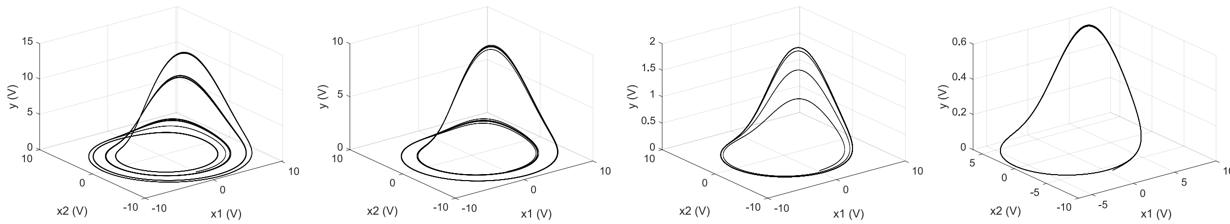

(a) $R_{a_1} = 650k\Omega$. (b) $R_{a_2} = 750k\Omega$. (c) $R_{a_3} = 1750k\Omega$ (d) $R_{a_4} = 3652k\Omega$

Figure 17: 3D results for increments in R_a.

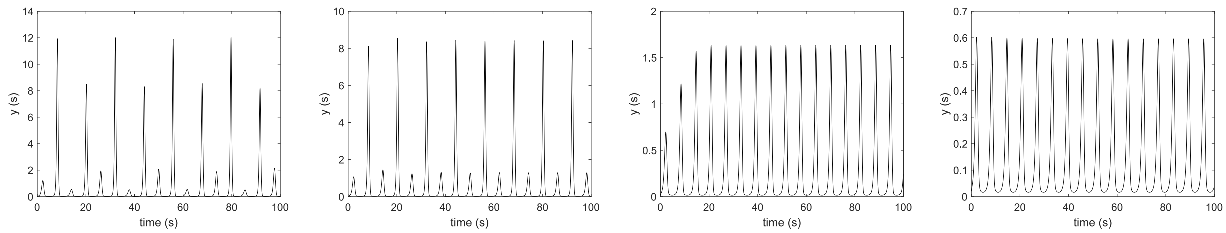

(a) $R_{a_1} = 650k\Omega$. (b) $R_{a_2} = 750k\Omega$. (c) $R_{a_3} = 1750k\Omega$ (d) $R_{a_4} = 3652k\Omega$

Figure 18: Output signal in time for increments in R_a

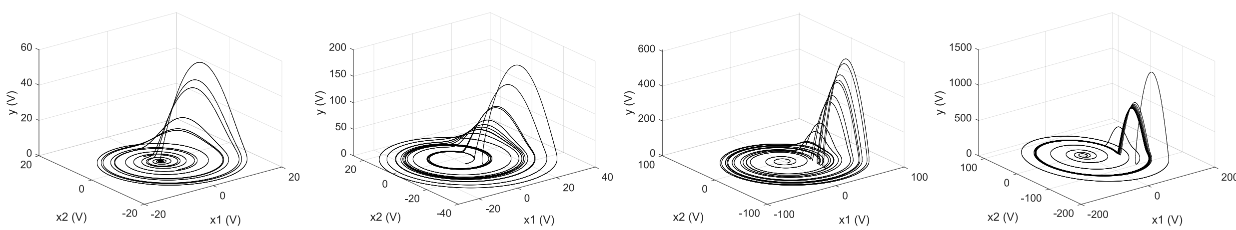

(a) $R_{c_1} = 10k\Omega$. (b) $R_{c_2} = 5k\Omega$. (c) $R_{c_3} = 2k\Omega$ (d) $R_{c_4} = 1k\Omega$

Figure 19: 3D results for smaller values of R_c.

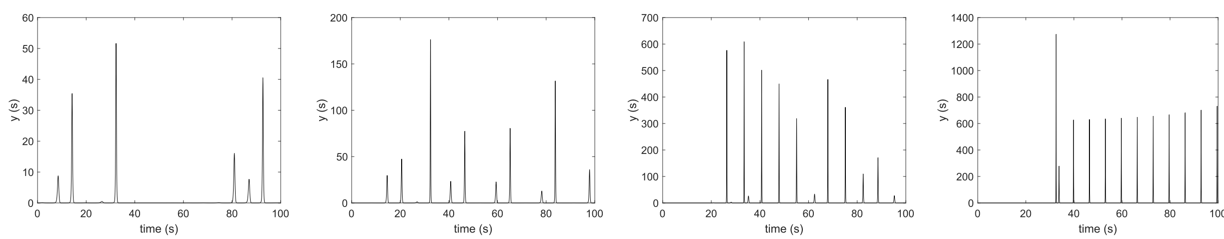

(a) $R_{c_1} = 10k\Omega$. (b) $R_{c_2} = 5k\Omega$. (c) $R_{c_3} = 2k\Omega$ (d) $R_{c_4} = 1k\Omega$

Figure 20: Output signal in time for smaller values of R_c

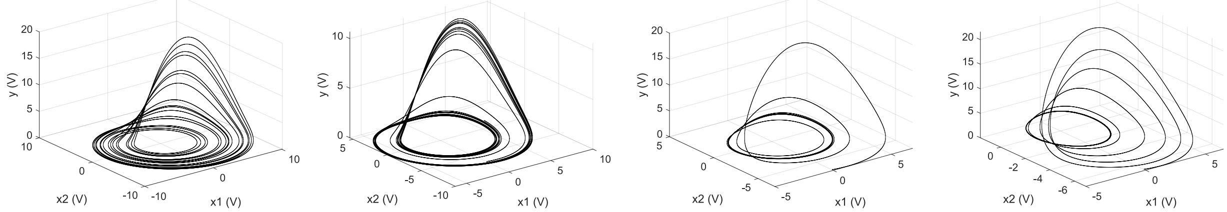

(a) $R_{c_5} = 20k\Omega$. (b) $R_{c_7} = 25k\Omega$. (c) $R_{c_7} = 50k\Omega$ (d) $R_{c_8} = 75k\Omega$

Figure 21: 3D results for increments in R_c.

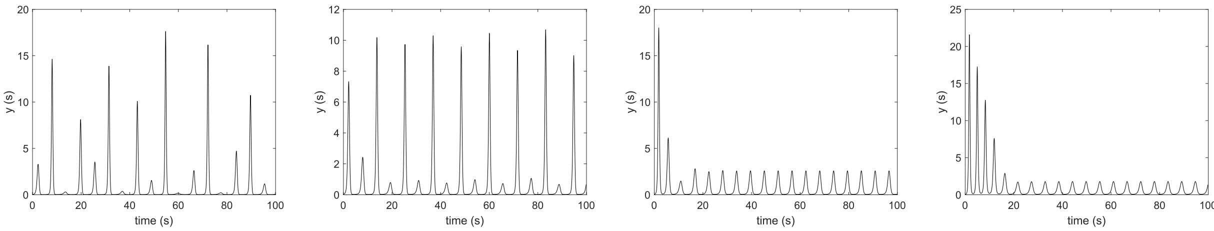

(a) $R_{c_5} = 20k\Omega$. (b) $R_{c_6} = 25k\Omega$. (c) $R_{c_7} = 50k\Omega$ (d) $R_{c_8} = 75k\Omega$

Figure 22: Output signal in time for increments in R_c

For the increment of R_a, the system behavior is periodic bounded by a decreasing signal, as the plot of y against time shows. The 3D plots shows that the orbit falls into a decreasing loop.

2) Parameter R_c: Following the idea from section III-D1, the found minimum found value for R_c is around $0.08400331675k\Omega$. In Figs. 27 and 28 the behavior of the output in time and all three variables is shown.

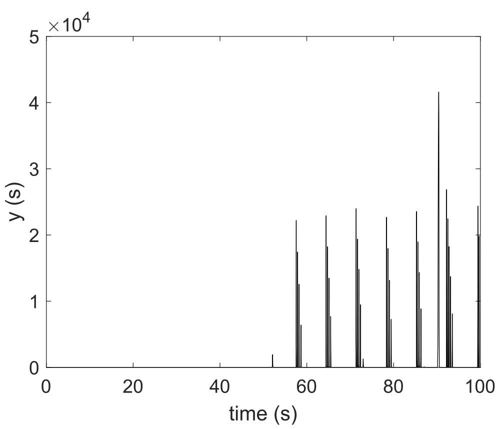

Figure 27: Output signal in significant time for reduction in parameter R_c.

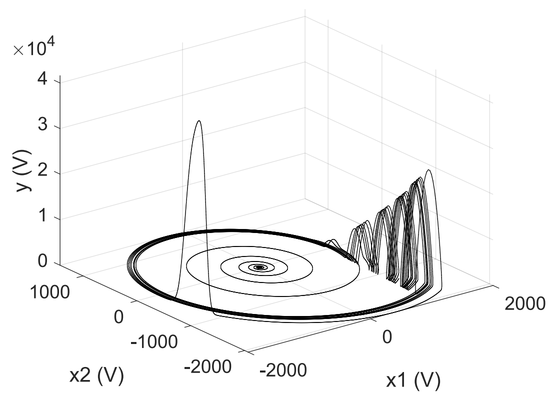

Figure 28: 3D phase plot for the state variables for a significant reduction in parameter R_c.

Notice that, in the 3D plot, the opening of the attractor is shrinked, compared to higher values for R_c. The peaks in the output signal are much bigger than the standard values (order of 10^4).

For the increment maximum value in R_c, around $88.48868k\Omega$ was found with the bisection method. In Figs. 29 and 30 the behavior of the output in time and all three variables is shown.

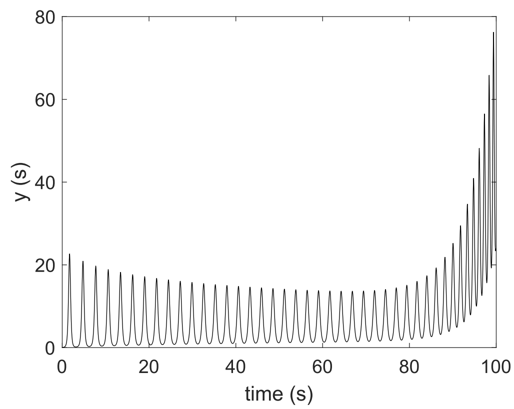

Figure 29: Output signal in time for a significant increment in parameter R_c.

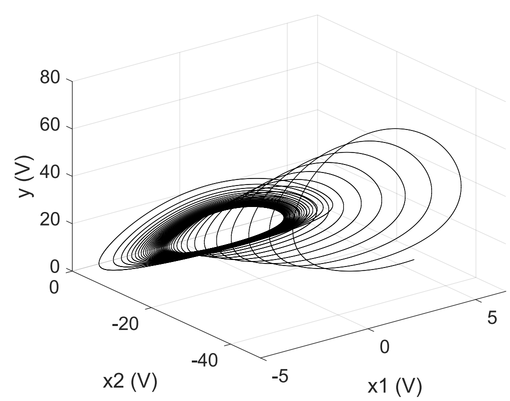

Figure 30: 3D phase plot for the state variables for an increment in parameter R_c.

E. Euler and Runge-Kutta Methods

A short comparison between the numerical methods was done, running simulations using Simulink's integrated methods and the manually programmed methods in Matlab for both fourth-order Runge-Kutta and Euler's method. The results are shown in Fig. 31.

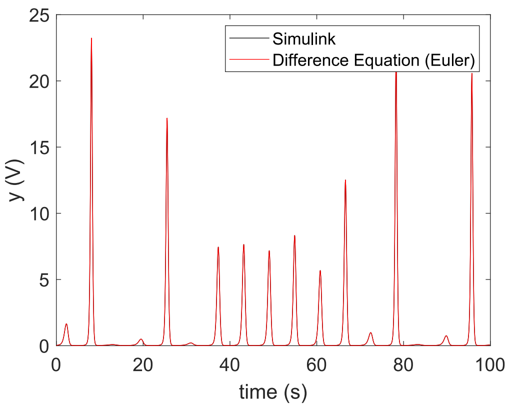

(a)

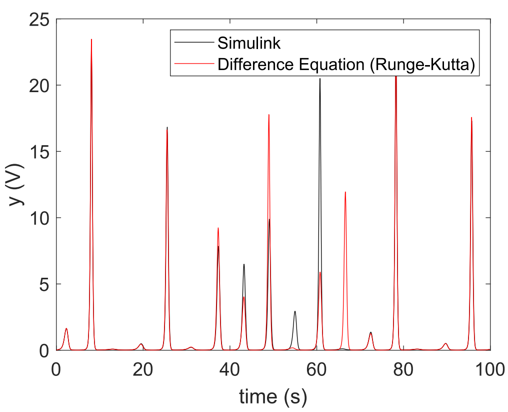

(b)

Figure 31: System simulation with both Runge-Kutta and Euler methods using Simulink and programming the difference equation.

IV. Results analysis

A. Model validation

As the previous section shows, every graph simulated in Simulink presents the same shape as the presented in the original articles, so the model used in this article is valid. Note that there are small differences with the maximum and minimum values that the voltages have and some trajectories that do not fit with the compared graphs. These differences occur due to several reasons that do not diminish the validation of the model. It is considered important to explain the reasons this differences may take place.

In first place, chaotic systems are highly sensitive to small changes in the parameters and initial conditions. The problem is when the system is simulated for every iteration it needs information of every state prior; and, if the system simulated is chaotic every minor approximation that the software makes for a certain iteration influence the posterior iterations value more heavily than other systems. Therefore, the chaotic nature of the attractor makes it difficult to replicate exact graphs from other work.

In second place, other articles do not specify what algorithm they used to solve their equation and, as it is seen in section III-E, the algorithm used to solve the differential equation affects the solution (specially if the system is chaotic as the equations used in this paper). And even if the algorithm is specified in the article, like in [1], the author do not specify the step that he used in the algorithm that also changes the simulation as seen in SECTION EULERDIFERENTEPASO.

Therefore, the problems explained are not related to the implementation of the model worked instead problems inherent to simulation of chaotic systems. Consequently, the model is validated.

B. Input Variation

1) Sines Inputs: As it was presented in section III-B1, both sine inputs make the system fall into a periodic orbit; this is due to the system no having enough time to create a chaotic behavior. It is constantly changing values from voltages that are known to cause chaotic behavior and some that do not. As the sine wave has an offset of $500V$, the average value is exactly $500V$; hence, as the input is much higher than the original V_{cc0} and then the circuit charges and discharges quite often.

Between the two simulations performed (Figs. 9 and 12), the sine input with less frequency (2rad $* s^{-1}$) could achieve a "simpler" orbit, since the system had a bit more time to attempt to follow an orbit alike the reference (Figs. 7 and 6; unlike the input with higher frequency, where the system immediately falls into a more complex orbit.

2) Step Input: As it is shown in section III-B2, the step input provides an effective controller for the system in stationary state. It can be observed that the output signal Fig. 16 stabilizes shortly after the input is applied; and as well for the phase portrait 15, since it converges to a point in space. The stabilization is a result of the circuit charging immediately: the voltage is so high that it will not create dynamic behavior through the nodes; it is constant.

C. Parameter Variation

It is important to highlight, that for the variation the parameters the values picked cannot be unusually big or small as resistance have a physical limitation for their values. In this manner, there is a threshold for what the minimum and maximum values can the resistances have without breaking the limitations of the system.

1) Parameter R_a: It is seen that as the value for the resistance a increases, the system changes for a more chaotic response to a periodic one as seen in figure 18. This result does not come as a surprise, as it is consistent with the known circuits theory. As R_a takes higher values, the current that moves around the circuit is lower due to the high resistance that the system has because of Ohm's Law. Therefore, the differences between the voltages in different times of the nodes are smaller, making the system periodic. Consequently, resistance a acts as a controller as for increasing values of this state variable the system easily starts to change its chaotic nature.

This characteristic is more evident when the system is simulated with the same parameters but, increasing the time of simulation as in figure 32. In this figure, the simulation is made with exactly the same parameters as in 17d but with the time of simulation 5 times the original. And, as it is seen, the graphic is totally identical to the original; then, this resistance makes the system completely oscillatory even for longer times therefore completely controlling it for increasing values.

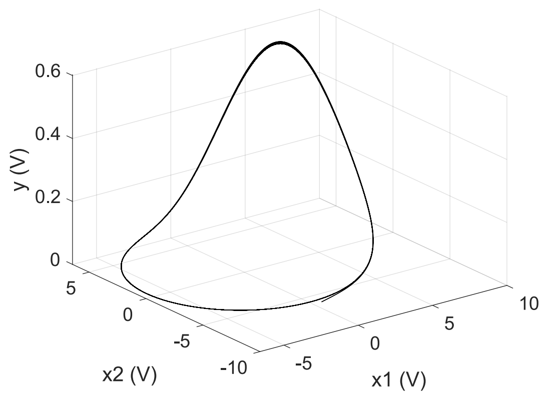

Figure 32: 3D results for R_a4 with final time 500.

2) Parameter R_c: For decreasing values of R_c it is seen that the values of the output increase. This is consistent with Ohm's law, as with lower resistance in the system the voltage is higher as there's more current in the circuit. In this manner, the first signal for y takes more time to show; however, the output signal, as stated in [5], is difficult to predict therefore understanding the nature of why this occur is almost impossible.

On the other hand, when the value of this resistance is increased it occurs a phenomenon similar with R_a but, instead of having an immediate periodic behaviour it has some high peaks at the start and then proceeds to control itself as in 22d. As stated before, the output signal is difficult to predict therefore is not possible to attribute why this peaks happen. Still, it is consistent that the voltage of the output becomes periodic and with small peaks for the same reason that with R_a.

Taking this into account, this resistance is harder to predict how it affects the system at the start but, when time passes it takes the expected behaviour. This happens because these parameter affects the non-linear equation, therefore changes done to its value does not make linear changes. On the other hand, R_a changes a linear equation making it quite easy to predict the changes that this value makes to the system.

D. Limit for Parameter Variation

1) Parameter R_a: As it is seen in 23 the output y have a increasing value, tending to infinity. This makes sense, as the resistance a is really low, therefore the same argument is applied as the one in the parameter variation. A analogous argument can be applied for the upper bound.

The problem with this found interval, is that it is known that this interval presents a range of values for which the system converges but, it is not sure that every value inside this range has a chaotic behavior. To found this interval it would be needed to make a partition of this interval with graphs with similar behaviour and, observe how chaotic is it (calculating the Lyapunov's Exponent) and categorizing it. But, the interval $[259.098131084k\Omega, 10000k\Omega]$ is a superset for the set of the values of R_a that makes the system keep its chaotic behaviour.

2) Parameter R_b: With this parameter, it can be argued similarly as the one before.

E. Euler's and Runge-Kutta's Methods

Section III-E shows the simulation results for both methods in both scenarios; Fig. 31. a) shows that, for the Euler method, the numerical solutions for the state equation are equivalent: both scenarios showed identical results since the output signals overlap.

For the Runge-Kutta's method, the results obtained are quite different. As Fig. 31 b) shows, both methods match on the peaks localization, but differ on their magnitude. Roughly, for $30s < t < 70s$, the difference can be easily perceived.

As it has been already explained, the main feature of chaotic systems is their sensitivity to small changes; the Runge-Kutta's algorithm has to do significantly more calculations, which implies that the propagation of error is much more notorious. As Simulink's implementation of this method is not known, it is tough to determine exactly what causes the difference with further implications; moreover, Simulink's method must have better handling of data and operations, since it must take advantage of the software features, and the algorithm implemented lacks efficiency.

V. Conclusions

In this work, the Rössler system was analyzed based on the circuit proposed by Canals *et al.*, simulated using Simulink and then the results were interpreted and justified. Regarding the goal of this research, values for both R_a and R_c which the system does not show desired behavior were successfully found, analyzing the system response to changes in these parameters, with the aid of bisection method. Regarding what was hypothesized, the first conjecture was wrong, as it was shown in section III-C1 and III-C2 and discussed in IV, since the response of the system remains chaotic for smaller values of the resistors. In contrast, the second conjecture was proven correct due to the fact that the step input, going from $0V$ to $1000V$, showed that the system stabilizes shortly after the input was applied, as shown in section III-B2 and discussed in IV-B2.

On the other hand, as the main objective was to find intervals where the system preserves its chaotic behavior, the procedure followed only allowed us to find an enclosing interval where the exact intervals must be, as this "critical" points are only near to values where the system loses its comprehensive behavior: for R_a, the enclosing interval shall be $[259.098131084k\Omega,\ 10000k\Omega]$ and for R_c is $[0.08400331675k\Omega,\ 88.38868k\Omega]$; in order to find an effective interval, more values for R_a and R_c should be tested and constantly checking for positive Lyapunov exponents [8], until a negative exponent is found since it yields the non-chaotic behavior.

REFERENCES

[1] O. E. Rössler, "An equation for continuous chaos," *Physics Letters A*, vol. 57, no. 5, pp. 397–398, 1976.

[2] M. K. Mandal, M. Kar, S. K. Singh, and V. K. Barnwal, "Symmetric key image encryption using chaotic rossler system," *Security and Communication Networks*, vol. 7, no. 11, pp. 2145–2152, 2014.

[3] D. S. Laiphrakpam and M. S. Khumanthem, "Cryptanalysis of symmetric key image encryption using chaotic rossler system," *Optik-International Journal for Light and Electron Optics*, vol. 135, pp. 200–209, 2017.

[4] J. Weule *et al.*, "Detection of n: m phase locking from noisy data: application to magnetoencephalography," *Phys. Rev. Lett*, vol. 81, no. 15, pp. 3291–3294, 1998.

[5] V. Canals, A. Morro, and J. L. Rosselló, "Random number generation based on the rossler attractor," *IEICE Proceeding Series*, vol. 1, pp. 272–275, 2014.

[6] J. Kiusalaas, *Numerical methods in engineering with python 3*. Cambridge University Press, 2013.

[7] J. C. Sprott and C. Li, "Asymmetric bistability in the rössler system." *Acta Physica Polonica B*, vol. 48, no. 1, 2017.

[8] G. Elert. Lyapunov exponent. [Online]. Available: https://hypertextbook.com/chaos/lyapunov-1/